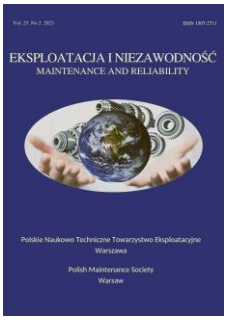

Eksploatacja i Niezawodnosc – Maintenance and Reliability
Volume 28 (2026), Issue 3
journal homepage: http://www.ein.org.pl

Article citation info:
Blaut J, Breńkacz Ł, Wróbel J, Drosińska-Komor M, Application of dispersion entropy in the diagnostics of a hydrodynamic bearing, Eksploatacja i Niezawodnosc – Maintenance and Reliability 2026: 28(3) http://doi.org/10.17531/ein/218330

Application of dispersion entropy in the diagnostics of a hydrodynamic bearing

Indexed by: Web of Science Group

Jędrzej Blaut[a], Łukasz Breńkacz[b,*], Jakub Wróbel[c], Marta Drosińska-Komor[d]

[a] Faculty of Mechanical Engineering and Robotics, AGH University of Krakow, Poland
[b] Institute of Fluid Flow Machinery, Polish Academy of Sciences, Poland
[c] Faculty of Mechanical Engineering, Wroclaw University of Science and Technology, Poland
[d] Faculty of Mechanical Engineering and Ship Technology, Gdańsk University of Technology, Poland

Highlights

- Dispersion entropy (DisEn) detects rotor imbalance in a hydrodynamic bearing.
- DisEn is evaluated from shaft displacement and bearing support acceleration signals.
- Experiments compare an unbalanced and an ISO-balanced rotor over 1,000–8,000 rpm.
- DisEn changes correlate with vibration amplitudes and orbital trajectories.
- The method is non-invasive and suitable for offshore and ship condition monitoring.

Abstract

This article presents a groundbreaking diagnostic methodology for detecting rotor imbalance in machinery through the innovative use of dispersion entropy (DisEn). Rotor imbalance, a prevalent issue in rotating machinery, greatly impacts operational efficiency, safety, and longevity, among others on the ship. The study proposes a non-invasive and highly sensitive method that uses DisEn to analyze vibration signals for the early and accurate detection of imbalances. The research includes a comprehensive experimental setup designed to simulate rotor imbalance conditions. DisEn, derived from Shannon entropy, offers a robust measure of signal complexity and irregularity, correlating with the severity of the imbalance. The study assesses DisEn values obtained from a rotor-bearing system's displacement and acceleration signals under various imbalance scenarios. The experimental results reveal that DisEn can effectively differentiate between balanced and unbalanced states at different operating speeds. This correlation is further substantiated by aligning with international rotor balancing standards, demonstrating the method's potential for real-time monitoring and diagnostics. The findings suggest promising opportunities for the broad application of DisEn in mechanical diagnostics, which calls for further research into its potential in different types of machinery and fault conditions. This methodology, along with the study's results, provides compelling evidence of the effectiveness and versatility of DisEn as a diagnostic tool, paving the way for its integration into modern diagnostic systems and the development of more reliable and efficient machinery.

Keywords
dispersion entropy, hydrodynamic bearing, vibration analysis, mechanical diagnostics, fault diagnosis

1. Introduction

Hydrodynamic bearings use a thin film of lubricant (such as oil or water) to create a film that supports the rotating shaft. This coating is created as a result of the movement of the bearing surfaces with lubricant, which creates pressure that keeps the surfaces apart [1]. The design and operation of this type of bearing is intended to ensure efficient and reliable operation of machinery, for example, a ship, turbine, or turbocharger [2]. As mentioned above, the basic principle of operation of

(*) Corresponding author.
E-mail addresses: J. Blaut (ORCID: 0000-0002-9638-1287) blaut@agh.edu.pl, Ł. Breńkacz (ORCID: 0000-0001-7480-9636) lbrenkacz@imp.gda.pl, J. Wróbel (ORCID: 0000-0001-6676-0051) jakub.wrobel@pwr.edu.pl, M. Drosińska-Komor (ORCID: 0000-0002-5614-1203) mardrosi@pg.edu.pl

a hydrodynamic bearing uses the hydrodynamic effect, which is the formation of a liquid film, the generation of pressure, and the retention of load retention [3]. The thickness and pressure depend on, among other things, the viscosity of the lubricant, the rotational speed, and the geometry of the bearing surface [4]. These bearings are used not only on ships but also in offshore systems.

In the ship, hydrodynamic bearings can be found in the propeller shaft which supports the propeller shaft, allowing it to rotate smoothly while transmitting power from the engine to the propeller. In this place, you usually use materials with high wear resistance and low friction, for example, bronze. Due to this, the bearing must accommodate large axial and radial loads, vibrations, and misalignments, so it is important to use diagnostic systems, an example of which is presented in this paper. In addition, they can be found in rudder bearings or turbomachinery bearings, which are devices responsible for ship propulsion, e.g. in turbines or compressors. Because they are in this place, they must provide high stability and low vibration to ensure efficient operation of the machinery. These bearings are used on ships because they can support significant loads and have a long life. Regular maintenance and monitoring are vital to ensure the longevity and reliability of hydrodynamic bearings on ships. In the next part of this work, we present our proposal about the diagnostic process.

In offshore applications, they have the same type of machinery as in ships. Here, they are used in various rotating machinery, such as turbines, pumps, and compressors. Due to the environmental conditions offshore, it is necessary to obtain the reliability, durability, and efficiency that are required. Therefore, when designing components of offshore equipment, it is necessary to use hydrodynamic bearings and monitor their operation. Hydrodynamic bearings can be found more precisely in offshore environments: turbomachinery, for example, in offshore platforms, drilling equipment, and subsea equipment (submersible pumps and motors). Importantly, they are characterized by low friction and low wear of the lubricant film, increasing efficiency. Furthermore, as previously mentioned, if proper lubrication is provided, hydrodynamic bearings can have a long service life. This is crucial because in offshore areas there are significant distances from the land, where maintenance is difficult and expensive.

Monitoring and diagnosing hydrodynamic bearings in see devices (e.g., ships, drilling platforms, offshore wind farms) is critical to ensuring the reliability and longevity of these objects. These bearings support essential elements such as propeller shafts or turbomachinery, where failures can lead to significant operational interruptions and breakage using this object. For this reason, the diagnostic method for hydrodynamic bearings will be presented in the next part of the work.

2. Diagnostics of a hydrodynamic bearing

Research into new methods of condition monitoring and fault diagnosis aims to prolong fault-free operation time [5]. This goal is being pursued through the development of precise hardware solutions [6], within the context of the Internet of Things [7], and using advanced signal processing techniques. Currently, there is a particular emphasis on non-linear analysis of diagnostic signals [8]. Bai et al. proposed a fault diagnosis method for rotating machinery based on SEDenseNet and Gramian angular field (GAF), to improve feature extraction and classification accuracy of characteristics [9]. GAF utilizes angular relationships between signal points to identify hidden fault characteristics, while the Squeeze and Excitation (SE) attention mechanism, combined with the DenseNet architecture, enables global information exchange and better multiscale fusion.

Lei et al. proposed a multiscale attention mechanism diagnosis method with an adaptive online update model based on deep learning to address challenges such as data drift and imbalance under variable operating conditions [10]. Kozłowski presented an assessment of maintenance system readiness using a semi-Markov model, considering the impact of hidden factors on reliability. The authors proposed a probabilistic analysis method that enables more precise modeling of degradation processes and maintenance strategies compared to traditional Markov models [11]. Borucka et al. examined lean manufacturing tools in production diagnostics, highlighting their role in efficiency improvement, failure detection, and reliability enhancement [12].

Analysis of operating parameters enables not only the current state of machinery but also the prediction of its future states. The prediction process is especially important in devices located at sea, where the diagnostic process is difficult to carry

out. This is so important because it allows you to plan necessary repairs to avoid failures. The fundamental principle of diagnostics is the postulate linking the increase in the level of vibroacoustic energy to operational wear. Therefore, it is essential to develop advanced diagnostic methods that precisely define the boundary between the useful state and the moment when continued machine operation becomes risky. This is especially important in the aspect of complex objects, e.g., ships or drilling platforms, where many elements can be damaged.

Imbalance is an important parameter that requires constant monitoring. Unwanted vibrations resulting from imbalance lead to higher energy consumption in mass production processing machinery, which in turn results in long-term economic losses [13]. In the case of ships, this is very unfavorable because it increases fuel consumption, resulting in higher production of CO_2, NOX, or SO_X [14]. This is a problem due to the requirements set by the authorities of countries around the world and the laws established by the world to limit greenhouse gas production [15,16].

Imbalance is a common issue in aircraft engine rotor systems or offshore wind turbines. A slight imbalance is unavoidable due to limitations in manufacturing precision. A dynamic balancing procedure is often necessary to minimize excessive imbalances. Imbalance can also result from damage to a rotating system, such as a propeller after a collision with a bird [17].

An imbalance in the context of machinery occurs when the mass of the rotor is unevenly distributed around the axis of rotation. An excessive imbalance can have serious consequences. An imbalance causes variable centrifugal forces during rotation, resulting in vibrations. These vibrations can accelerate machinery wear, shorten its useful life, and increase the risk of damage. Imbalance can induce structural resonances, potentially compromising structural integrity. The solution to all these problems is to perform a balancing process, precisely adjusting the mass distribution of rotating parts to reduce centrifugal forces, that is, evenly distributing the weight to minimize the forces that act on the rotating system. This is especially important for machines such as rotors, shafts, flywheels, or turbines that achieve high rotational speeds; these devices are broadly understood offshore.

Therefore, effective methods for detecting and monitoring imbalances. These methods should be able to identify and monitor even a small value of the imbalance without interfering with the normal operation of the machine.

Rotor imbalance occurs when the distribution of the mass along the axial section of the rotor in the radial direction is unequal. As a result, the geometric centerline of rotation does not coincide with the rotor's centerline of inertia mass. Fig. 1 illustrates the imbalance condition of the rotor when it rotates at a constant speed. It can be observed in the figure that the imbalance force is a centrifugal force synchronized with the rotational speed (synchronous rotational force). This force depends on the eccentricity, which is the distance of imbalance from the rotor axis. The basic model describing the radial vibration caused by mass imbalance forces is represented as:

$$\begin{aligned} m_t\ddot{x}(f) + d_x\dot{x}(t) + k_x x(t) &= m_e r\omega_r^2 cos(\omega_r t - \delta) \\ m_t\ddot{y}(f) + d_y\dot{y}(t) + k_y y(t) &= m_e r\omega_r^2 sin(\omega_r t - \delta) \end{aligned} \quad (1)$$

Where m_t is the mass, d is the damping coefficient, and k is the stiffness coefficient. Damping and stiffness are parameters of bearings; they depend solely on the coupling between the rotor and its supports. The magnitude of the imbalance force is proportional to m_e, where m_e is the imbalance mass, and $\boldsymbol{F} = m_e \cdot r$ is the imbalance. Imbalance is a vector quantity with a specific direction and magnitude, represented by the vector of the imbalanced centrifugal force F. Equation (1) shows the relationship between the imbalance force and the transverse vibration of the rotor. A simple rotor, supported by two bearings with a disk in the center, whose motion can be described by the equation shown, is called a Jeffcott rotor [18].

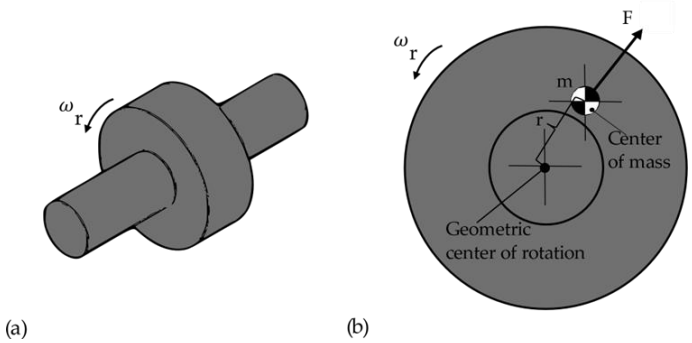

Figre 1. Imbalance scheme: (a) conceptual view of an unbalanced disc rotor; (b) cross-section showing the imbalance mass m and eccentricity r between the geometric centre of rotation and the centre of mass.

The operation of sliding bearings can exhibit strong non-

linearity. The source of such non-linearity can be, for example, bearing wear. This is particularly important in ships because plain bearings play a key role in the functioning of many systems on ships (drive shafts, turbines, generators, and hydraulic systems), providing support and reducing friction between moving elements. Due to their simple structure, plain bearings are resistant to heavy loads and unfavorable working conditions, which often occur on ships. In the context of technical diagnostics, there is a clear demand for methods that effectively address these non-linear aspects, enabling more precise monitoring of machine conditions and prediction of potential malfunctions.

These methods can be divided into many categories, each offering unique advantages and targeting specific aspects of signal analysis for fault diagnosis and condition monitoring in mechanical systems. One such category includes techniques based on the Teager-Kaiser energy operator, which has shown effectiveness in identifying energy dissipation and nonlinear dynamics within mechanical systems [19]. This approach is particularly useful for capturing the instantaneous energy of signals, providing a deeper understanding of operational health without the need for extensive signal processing [20].

Another noteworthy method involves linearizing non-stationary signals to facilitate their analysis. Burdzik [21] Discusses the adaptation of linear decimation procedures for the analysis of non-stationary vibration signals, particularly in vehicle suspensions. This approach aims to simplify the complex and time-varying nature of these signals, making it easier to identify anomalies and predict system failures.

Time-frequency decomposition techniques, such as empiric mode decomposition, as explored by Antoniadou [22] offer a powerful tool for decomposing complex signals into simpler intrinsic mode functions. This method is particularly effective in analyzing non-linear and non-stationary signals commonly encountered in wind turbine gearboxes, allowing for a detailed understanding of the system's dynamic behavior under varying load conditions.

Fuzzy theory, introduced by Song [23], employs fuzzy logic to handle uncertainty and imprecision inherent in diagnostic signals. This method enables the effective diagnosis of equipment conditions by extracting symptoms and applying trivalent logic fuzzy diagnosis theory, thus providing a more intuitive understanding of the system's health.

Sparsity theory, as discussed by Hao [24], applies sparse representation to fault diagnosis, allowing efficient analysis of signals by identifying sparse components that are indicative of system faults. This approach has proven useful for diagnosing compound faults in mechanical systems using geometric features.

Morphofiltering, presented by Li [25], uses morphological filters to extract noise and features in signal processing. This technique is particularly adept at enhancing the diagnostic capability of systems by improving the clarity and reliability of signal features related to faults.

Lastly, the application of machine learning in fault diagnosis, as investigated by Pawlik [26], represents a significant advancement in the field. Using artificial neural networks that do not require training data from faulty machines, this approach offers a flexible and powerful tool to diagnose faults in machines operating under variable conditions, highlighting the potential of machine learning to automate and improve the accuracy of diagnostic processes.

Collectively, these methods underscore the diverse and multifaceted approaches available for diagnosing and monitoring the condition of mechanical systems. It is especially applicable in multi-device technical facilities such as ships or drilling platforms. Each technique, with its unique strengths and applications, contributes to the broader objective of improving the reliability, efficiency, and safety of machinery operations.

Research is also being conducted on an innovative turbogenerator capable of operating at very high rotational speeds, with bearings that do not require oil lubrication. In addition, investigations are underway on an innovative turbogenerator designed to operate at extremely high rotational speeds, featuring oil-free bearings [27,28]. The research aimed to examine the impact of individual components on the dynamics of a prototype microturbine and to identify interactions between them. In addition to studies conducted on the high-speed rotor and bearings, the analysis also considered the dynamic properties of the supporting structure, comprising the casing, steel base plate, and frame [29]. Simulations allow analyzing the performance of such a machine by presenting the shaft vibration amplitude as a function of rotational speed, as the results of the modal analysis that illustrate the natural

vibrations of the system and their corresponding frequencies [30].

A promising approach in the field of vibroacoustic diagnostics is the use of dispersion entropy [31]. This article discusses experiments to evaluate the effect of rotor imbalance on the dispersion entropy value determined from the displacement and acceleration signals.

To assess the condition of a machine in terms of the magnitude of the imbalance, relevant standards are commonly utilized. The Standards of the International Organization for Standardization (for example, ISO 21940-11:2016 [32]), precisely regulate acceptable imbalance conditions for various applications. They provide guidelines for rotor balancing methods, encompassing various aspects such as definitions of imbalance, estimation of imbalance based on mechanical vibration, balancing techniques for different rotor configurations, and considerations of imbalance for machines operating at single and multiple speeds. Moreover, these standards precisely define maximum imbalance values for various applications, taking into account the rotor speed.

Advanced applications use systems such as high-speed field-programmable gate arrays (FPGAs), 3D scanners, and digital signal processors for real-time vibration monitoring and active imbalance control. In a paper [33], we presented a novel adaptive vision method for the automatic detection of rotor imbalance. The online implementation of this method has been shown to enable real-time rotor balancing. The proposed solution integrates 3D sensors into a dynamic balancing platform, employing 3D computer vision technology and a dynamic balancing algorithm to improve the efficiency of the dynamic balancing process. In such applications, estimation and correction are performed in real-time through a user interface, using a feedback loop with sensors and actuators [34].

Physical model-based techniques use simplified rotor models to estimate the imbalance, relying on physical principles related to the mechanical interaction between the components of the system. The imbalance is estimated in the model and the data are collected from the sensors. A paper [35] discusses the modeling, analysis, and identification of finite element models of a flexible levitating rotor with faults using active magnetic bearings. A flexible axle with an imbalanced rotor, consisting of multiple disks lifted by a set of off-axis active magnetic bearings, was mathematically modeled using the finite element method with Timoshenko-type beam elements [36]. Although such applications have been shown to effectively detect imbalance in both experimental and simulated configurations, the drawback lies in the time and effort required to perform finite element analysis for each rotor under study (rotor-stator system, rotor system), which limits their implementation.

In summary, a deeper understanding of the details of rotor-related operations is needed, which can be challenging in practice. Furthermore, the dynamic response of the rotor, as determined by the finite element method, may change during operation [37].

The main achievement presented within the framework of this work is an innovative methodology for monitoring rotor imbalance. It uses the key advantages and complementarity of signal processing techniques and system identification algorithms to effectively solve the imbalance monitoring problem. The methodology also features a non-invasive approach, as it requires only the use of a speed sensor and eddy current sensors mounted on two rotor brackets. Note that these sensors are often standard tools for analyzing the operation of rotating machinery.

3. Dispersion entropy

Dispersion entropy (DisEn), based on Shannon's entropy, is a tool for the rapid measurement of irregularities. The concept of symbolic dynamics stems from the simplification of measurements, in which a time series is transformed into a new signal that contains only a few different elements. Analyzing signal dynamics involves examining a sequence of symbols, which can lead to loss of some detailed information, but simultaneously preserves certain robust features of dynamics [38]. DisEn is used on ships where complex mechanical and electronic systems are exposed to extreme operating conditions. In this case, DisEn can play a key role in the process of monitoring the technical condition of systems and diagnosing failures of devices on ships. DisEn is particularly effective in evaluating complex and complex data, which is often encountered in real operational conditions.

Recent studies have highlighted the effectiveness of dispersion entropy in the diagnosis of bearing failures. Zhang et al. introduced hierarchical dispersion entropy (HDE), which

outperforms traditional methods by accurately distinguishing various types of rolling bearings [39]. Similarly, Li et al. developed a fractional order fuzzy dispersion entropy, which improves sensitivity to dynamic changes in time series, achieving a 100% recognition rate in fault diagnosis [40]. Blaut and Breńkacz explored the application of dispersion entropy with a sliding window, emphasizing its utility in assessing machine stability and the importance of window length for effective diagnostics [41]. Collectively, these studies underscore the potential of dispersion entropy techniques to improve machine diagnostics, particularly in bearing applications.

The best-known methods based on symbol entropy are approximate entropy, permutation entropy, and DisEn, which are used in this paper. DisEn represents an innovative approach to monitoring the imbalance in temporal signals. In the context of analyzing one-dimensional signals of length N, represented by a time series x = x1, x2,..., xN, the determination of DisEn involves four main steps:

Step 1: Assign elements x_j (j = 1,2,..., N) to classes c using a series of linear and nonlinear approaches. To do this, one typically employs the normal distribution function and then uses a linear algorithm to assign values y = y1, y2,..., yN in the range of 0 to 1. This step enables efficient classification of time series elements and can also be executed using other linear and nonlinear mapping techniques.

Step 2: Determine possible dispersion patterns by creating embedding vectors mc_i^z, where each vector has an embedding dimension -emb_dim and a time delay. From these vectors, a dispersion pattern $\Pi^{memb\_dim-1}\Pi$ is formed. Each time series $z_i^{emb\_dim,\, classes}$ is mapped to a dispersion pattern, which is used for further analysis.

Step 3: Count the frequency of occurrence for each potential dispersion pattern. This calculation involves determining the relative frequencies of each possible pattern.

Step 4: Calculate the entropy using Shannon's definition of entropy. The resulting entropy value DE(x_j, *emb_dim*, *classes*, *delay*) reflects the degree of chaos and unpredictability of the signal depending on the embedding dimension (*emb_dim*), the time delay (delay) and the number of classes.

The parameters of DisEn, such as the embedding dimension (*emb_dim*), the number of classes (*classes*), and the time delay (*delay*), must be selected accordingly. For example, applying DisEn to the study of hydrodynamic stability in sliding bearing operation resulted in the selection of parameters: *classes* = 10, *emb_dim* = 2, *delay* = 1. The optimal choice of parameters affects the efficiency of the method and the stability of the results obtained, eliminating potential distortions and errors. Based on a study on the application of DisEn in rolling bearing analysis [31], parameters such as *classes* = 10 were selected in the context of testing the rotor imbalance.

For a class parameter that is too small, two very distant amplitudes can be erroneously assigned to a similar class; for a large c, even a small change can affect the class change, making the method sensitive to noise. In addition, excessively high values of *m* or *c* increase the computational time. A large embedding dimension *m* may hinder the DisEn algorithm in detecting subtle changes. The parameter *emb_dim* = 2 was chosen.

The study confirmed that with a small embedding dimension *m* and a large number of classes *c*, DisEn gives more reproducible results. The stability of DisEn -based profiles increases with the length of the signal, which led to the use of *m* = 2 in the studies carried out. Parameter *delay* = 1 was selected.The time delay (*delay*) exceeding a value of 4 causes the standard deviation of DisEn in the signals to be higher. In this study, a delay time = 1 was used.

4. Experimental studies

A research station designed to examine small rotors has been developed to facilitate the investigation of a rotor bearing system, focusing on identifying and studying various defects, including bearing failure, rotor imbalance, misalignment, etc. With the supporting frame, the assembly weighs approximately 60 kg.

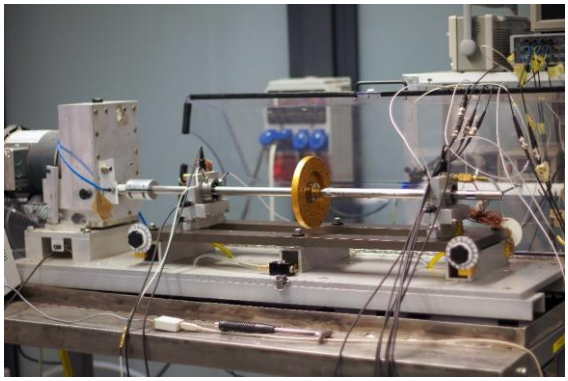

Figure 2. Photo of the laboratory station.

Fig. 2 illustrates the layout of the experimental stand, detailing its dimensions and key components. The stand measures 125 cm in length, 36 cm in width, and 65 cm in height. Additionally, the figure outlines the coordinate system applied during the experimental procedures. The foundation of the laboratory stand comprises a 13 mm thick steel plate, onto which two channel bars are mounted to facilitate height adjustment and ensure level positioning. The rotor is secured within two bearings and is propelled by a 3-phase motor with a maximum speed of 3,450 rpm, regulated by an inverter with a capacity of 1.5 kW. This motor is linked to a gearbox that amplifies the rotational speed approximately 3.5 times, allowing a maximum speed of 12,000 rpm. The dimensions of the coupling are 50 mm in diameter and 60 mm in length. A pump capable of producing a maximum of 35 PSI (0.24 MPa) supplies oil to the bearings, with the pressure maintained at 23 PSI (0.16 MPa) during experiments.

The tested rotor has a length of 920 mm. The space between the coupling and the nearest support is 170 mm, with the rotor positioned between two bearing supports. The total distance spanned by the supports is 580 mm, with bearings numbered 1 (near the motor) and 2 (opposite side). The rotor disk is located equidistantly between the supports, making the lengths l1 and l2 identical, as shown in Fig. 3. The rotor diameter measures 19.02 mm, while the disk diameter is 152.4 mm. Displacement sensors, specifically uniaxial for bearing supports and eddy current sensors at points D_1 and D_2, are strategically placed to measure displacement on both the X and Y axes, with respective distances of 20 mm and 30 mm from the bearing centers. This arrangement is due to the operational requirements of eddy current sensors, which cannot function in the same plane and are positioned at a 90 degree angle to each other, aligning 45 degrees with the reference system. To ensure operational safety, a clear plastic envelopes the rotor bearing system. During the measurements, four Sinocera CWY-DO-501A eddy current sensors (sensitivity: 4 mV/µm; measurement range: 0–1 mm), four PCB 608A11 uniaxial accelerometers (sensitivity: 100 mV/g; range: ±50 g), and a laser tachometer (Optel Thevon 152 G7) were integrated with LMS SCADAS data acquisition hardware.

Both hydrodynamic bearings supporting the rotor share the same geometric specifications, with a lubrication gap of 76 µm relative to the shaft radius. The bearing length is 12.6 mm. Lubrication is delivered through two holes on either side of the shaft, each with a diameter of 0.1 ″ (2.54 mm), using oil of the ISO 13 viscosity class.

The test stand is designed to enable precise control of rotor imbalance by incorporating threaded inserts of known mass and location into the rotor disc. Rotor balancing was performed in accordance with ISO 1940-1:2003, achieving a G6.3 balance quality grade at a maximum speed of 8,000 rpm. To simulate an imbalanced condition, additional mass was deliberately added to the rotor disc, creating a specific unbalance equivalent to twice the permissible residual level for the G6.3 grade.

4.1. Displacement

Displacement was measured at three points (D_1, D2, and D3 discs) marked on the diagram below (Fig. 3).

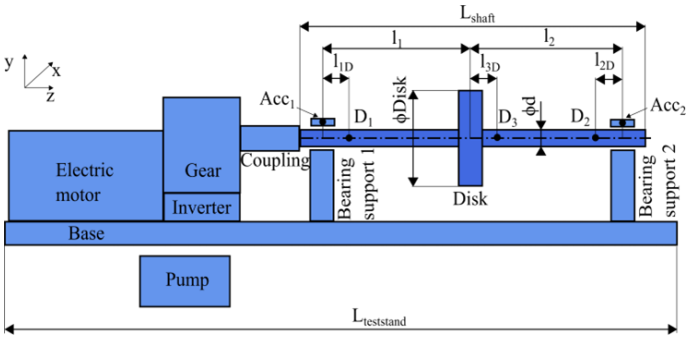

Figure 3. Schematic of the laboratory setup.

At each of these measurement points, the displacement was recorded on the two x- and y-axes. The length of the resultant vector was then calculated as $\|d\| = \sqrt{d_x^2 + d_y^2}$, representing the physical maximum deflection of the shaft from the averaged center of the shaft. Fig. 4 shows the maximum displacement for the given rotational speeds, which determines the maximum deflection of the shaft from the center of rotation. The data series correspond to vibration parameters registered at three measurement points: D1, D2, and D3. The first point is marked with a dot and colored blue for the experiment with an imbalanced rotor, and dodger blue for the experiment with a balanced rotor. The second measurement point is marked in dark orange for the experiment with an imbalanced rotor and in gold for the experiment with a balanced rotor. The measurement spot close to the disc, labeled ‘rotor’, is marked in forest green for the experiment of the imbalanced rotor and in lime green for the experiment of the balanced rotor. In addition, they have different markers: dot, triangle, and square to make it easier to

read the relationships. Generally, dark colors correspond to the experiment before the balancing process, and light colors correspond to the experiment after the balancing process. The balance process reduced the centrifugal force resulting from the uneven distribution of the mass in the rotor. This translated into an apparent reduction in the amplitude of vibration displacement of the rotor disk at almost every measurement point. The largest displacements were recorded between the bearings at the disc location. The largest decrease in the amplitude of the vibration displacement after the balancing process is also visible at this location. The percentage decrease is marked on the graph. For example, at a speed of 5000 rpm in Fig. 4, a 22% decrease in value after balancing is marked with a red arrow. The smallest differences were observed for rotational speeds from 1000 to 3000 rpm and from 7000 to 8000 rpm. For the experiment, the most interesting observation is the location at the rotor for speeds from 4000 to 7000 rpm. In the displacement diagram, you can find three instances in which there was no decrease in displacement amplitude after the balancing process. D1: 1000 rpm; D2: 1000 and 2000 rpm.

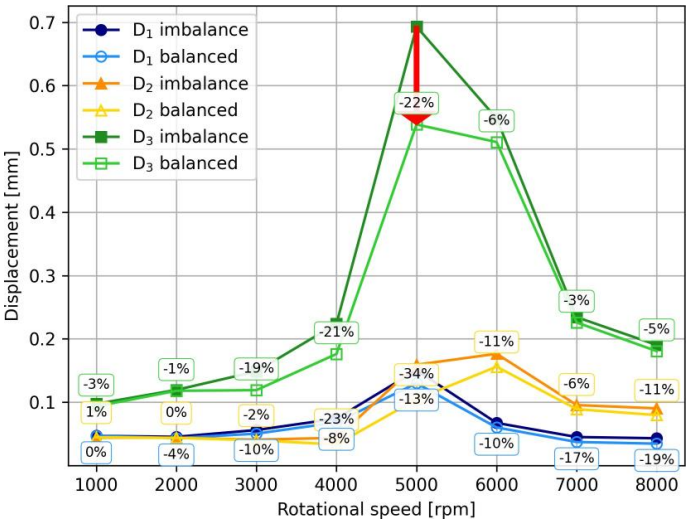

Figure 4. Displacement versus rotational speed for the unbalanced and balanced rotor.

4.2. Acceleration

Acceleration was measured at the two measurement points shown in the diagram. At both points, acceleration was recorded on the x- and y-axes. The length of the resultant vector was then calculated as $\|a\| = \sqrt{a_x^2 + a_y^2}$. The registered acceleration made it possible to compare the effectiveness of detecting system instability using DisEn with respect to the expected increase in vibration acceleration. Acceleration signals are taken into account to detect the imbalance and evaluate its magnitude with respect to the relevant standards. This allows appropriate remedial action to be taken, such as the addition of counterweights or other procedures to correct the rotor balance problem. Fig. 5 shows the acceleration of vibration recorded by accelerometers placed on the bearing supports. The tests were carried out for two values of rotor imbalance, similar to the displacements described above. Similar graphical designations were used to improve the readability of the graph. Significant decreases in vibration acceleration values can be seen at both measured points. Differences are visible only above a rotational speed of 4000 rpm. In the case of the observation of displacement amplitude, the values before and after the balancing process already differed from 3000 rpm. In the graph showing acceleration, it is possible to find seven rotor speeds for which there was no decrease in vibration acceleration values after the balancing process: Acc_1: 1000, 3000, 4000 rpm, Acc_2: 1000, 2000, 3000, 4000 rpm.

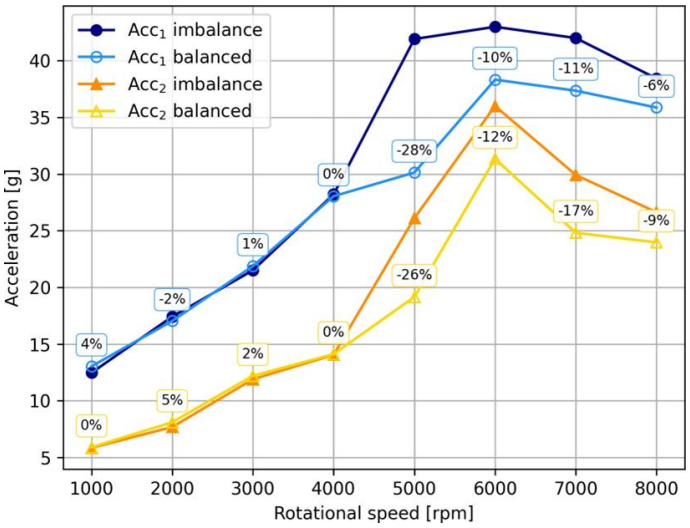

Figure 5. Acceleration depending on the rotational speed for the unbalanced and balanced rotor.

4.3. DisEn calculated from displacement

DisEn in the study was calculated on the displacement signal described in Section 3.1. Fig. 6 shows the DisEn values determined for the displacement signals registered at three measurement points: 1, 2 and Rotor, before and after the balancing process, as a function of rotational speed. Separately, the value of DisEn was determined for the x and y axes, and then the length of the resultant vector was calculated as

$\|DisEn\| = \sqrt{DisEn_{dx}^2 + DisEn_{dy}^2}$. Because of the similar values for the three measurement locations, the graphs showing DisEn determined from displacement were separated into a series of three graphs. The designations in symbols and colors correspond to the signals from which they were determined (Fig. 4). It can be seen that the value of DisEn increases after the balancing process. In practice, a high DisEn value indicates a high irregularity or complexity of the signal. However, in the experiment, the opposite correlation was observed. After the balancing process, the value of DisEn increases. In the graph showing the DisEn calculated from the displacement signal, you can find seven cases in which there was no increase in the value after the balancing process. D_1: 1000, 2000 and 3000 rpm; D_2: 4000 and 6000 rpm; D_3: 1000 and 3000 rpm.

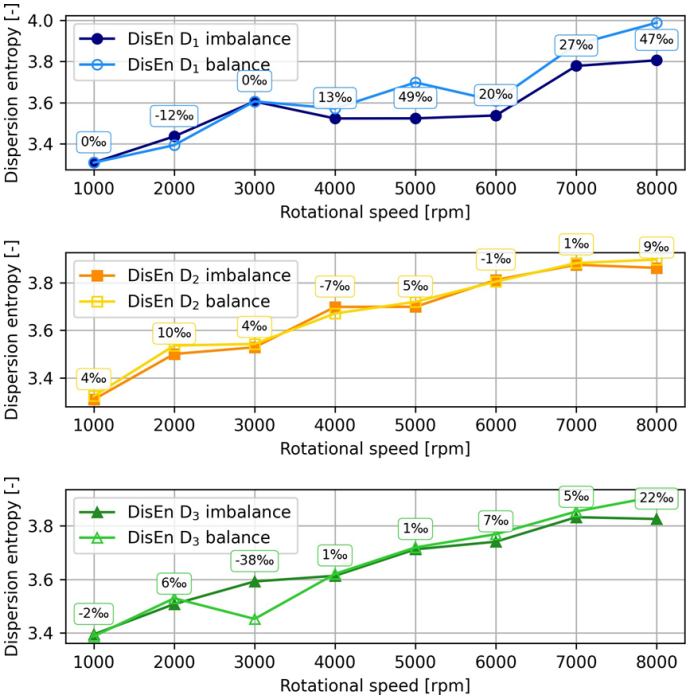

Figure 6. Dispersion entropy as a function of rotational speed for the unbalanced and balanced rotor based on displacement signal.

4.4. DisEn calculated from acceleration

DisEn in the study was also calculated based on the acceleration signal described in Section 3.2. Fig. 7 shows the DisEn values determined for the acceleration signals at the two measurement points, before and after the balancing process, as a function of rotational speed. Separately, the value of DisEn was determined for the x and y axes, and then the length of the resultant vector was determined as $\|DisEn\| = \sqrt{DisEn_{accx}^2 + DisEn_{accy}^2}$. The markings in the form of symbols and colors correspond to the signals based on which they were determined (Fig. 5). It can be observed that the value of DisEn increases after the balancing process, similar to what occurred when DisEn was determined from the displacement signal. Once again, an intuitively opposite correlation of DisEn values was observed in the experiment before and after the balancing process. An increase in DisEn values after the process indicates an increase in the irregularity and complexity of the acceleration signal. In the graph showing DisEn calculated from the displacement signal, one can find four cases in which its value did not occur after the balancing process: Acc_1: 2000 and 3000 rpm, Acc_2: 4000 and 6000 rpm.

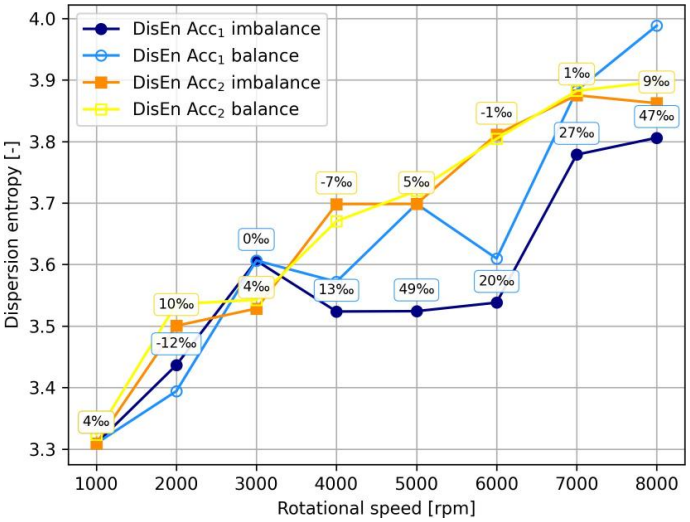

Figure 7. The dispersion entropy depends on the rotational speed of the unbalanced and balanced rotor based on acceleration signals.

5. Discusion

For an explanation of the experimental results, a comparison of the displacement trajectories obtained for two of the measurement locations before and after the balancing process was carried out for different speeds was carried out. The displacement trajectory is used for bearing diagnostics. When the x- and y-axes displacement signals on the x- and y axes are assembled at a given measurement location, we can trace the movement of the center of the shaft relative to the displacement sensors.

The first case analyzed is the shape of the rotational trajectory at measurement site 1 at 5000 rpm, where the DisEn difference after the balancing process was equal to +4.9%. Fig.

8 shows the plots of the rotational trajectory at measurement location 1 for a rotational speed of 5000 rpm before and after the balancing process. The operation of sliding bearings after the balancing process has a similar shape, but is "narrower". Additionally, the subsequent trajectories are closer together and the trajectory trace is thinner. Despite this, the value of DisEn increases, which is counterintuitive. In the second case, the shape of the rotational trajectory was analyzed at the measurement point close to the disk at 3000 rpm, where the value of DisEn decreased by 3.8% (-3.8%) after the balancing process. Fig. 9 shows the plots of the rotational trajectory at the measuring point near the disk for a rotational speed of 3000 rpm before and after the balancing process. It can be seen that the trajectory after the balancing process has a similar shape but is "narrower". Additionally, the subsequent trajectories are further apart, and the trajectory trace is wider.

According to this approach, it can be seen that DisEn has a higher value when the analysis is more recurrent, which contradicts the definition of Information Entropy. However, this does not disqualify the use of DisEn-based methods in imbalance diagnostics because the essence is to observe a change in the value of the parameter being evaluated. The article uses the parameters described in Chapter 2 and drawn from previous research; it is undeniable that the selection of different parameters could affect the results of the determination of DisEn.

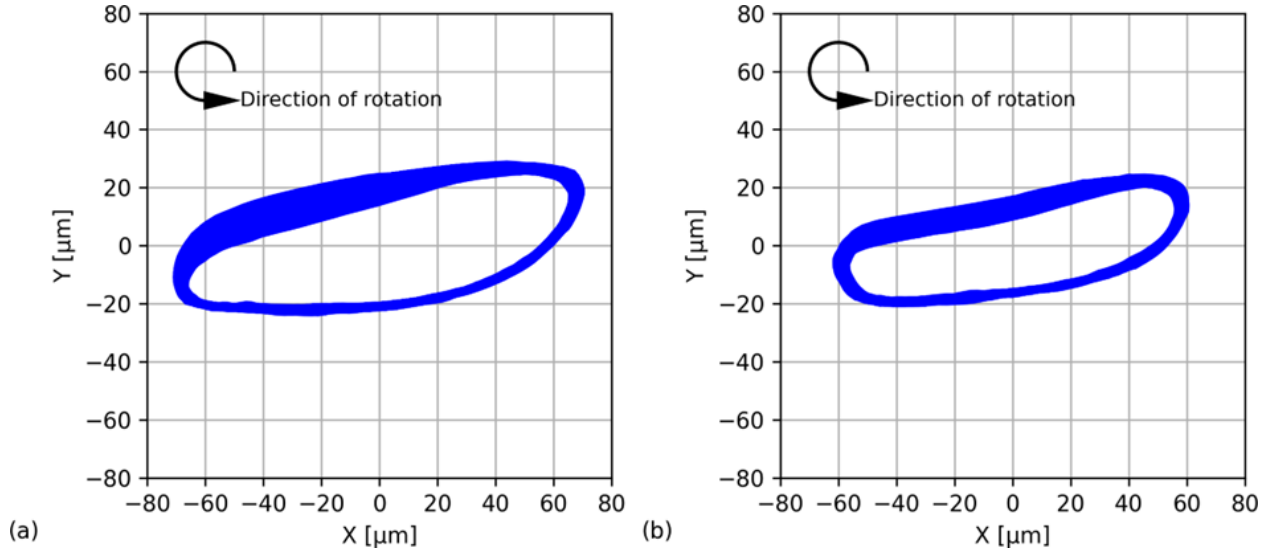

Figure 8. Diagrams of the rotational trajectory at measurement point 1 for a rotational speed of 5000 rpm (a) before and after (b) the balancing process; DisEn value is + 4.9%.

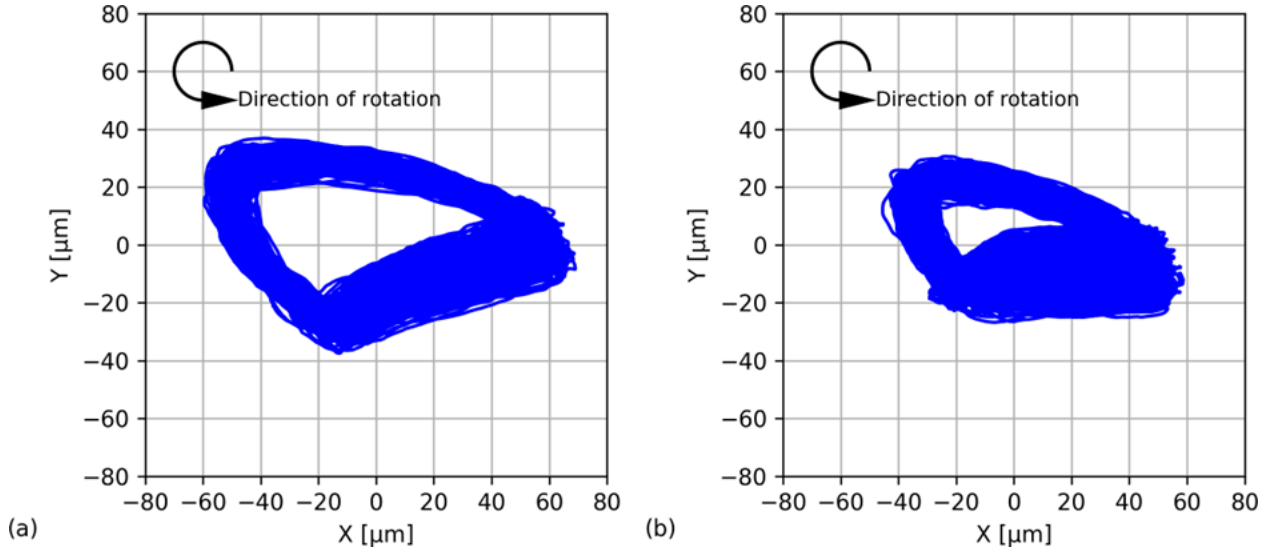

Figure 9. Charts of the rotor trajectory at the measurement point close to the rotor for a rotational speed of 3000 rpm (a) before and

(b) after the balancing process; the DisEn value is -3.8%.

6. Summary and conclusions

Technological advances in machine diagnostics enable the development of analytical methods that facilitate complete analysis of diagnostic parameters. This, in turn, allows rational decisions about the technical condition of the equipment. This is very important in the case of ships, where failures can lead to their discontinuation or long repair times, which results in a loss of money for the shipowner, which is why it is so important to carry out the diagnostic process in such facilities, Or in other devices operating at sea, because they are located far from land, which makes their inspection and maintenance difficult. In advanced diagnostic systems, the number of measurement sensors is increasing, and we also have increasingly sophisticated algorithms to interpret measured signals. It is becoming standard to determine trends and warning values. This research proposes a method based on diffusion entropy to assess rotor imbalance by studying two configurations of the system: before and after balancing. The results of DisEn analyzes for the two imbalance cases were compared with measured rotor displacements and bearing support accelerations. Furthermore, the vibration trajectories clearly show the differences between balanced and unbalanced systems. These differences are evident for all the signals analyzed, demonstrating that DisEn can be used effectively to assess the imbalance. The DisEn method can also be used to find correlations using long-term statistical data.

The results obtained from the experimental research are promising and indicate the need for further study of the potential application of DisEn in diagnosis within a broader diagnostic context. An important aspect of such a study is determining the minimum signal length required to achieve stable results of the DisEn values.

References

1. Głuch J. Fault detection in measuring systems of power plants. Polish Maritime Research 2008; 15(3): 45–51. https://doi.org/10.2478/v10012-007-0096-8.
2. Liu W, Ni H, Wang P, Chen H. Investigation on the tribological performance of micro-dimples textured surface combined with longitudinal or transverse vibration under hydrodynamic lubrication. International Journal of Mechanical Sciences 2020; 174: 105474. https://doi.org/10.1016/j.ijmecsci.2020.105474.
3. Pfeil S, Gravenkamp H, Duvigneau F, Woschke E. Scaled boundary finite element method for hydrodynamic bearings in rotordynamic simulations. International Journal of Mechanical Sciences 2021; 199: 106427. https://doi.org/10.1016/j.ijmecsci.2021.106427.
4. Pfeil S, Gravenkamp H, Duvigneau F, Woschke E. Semi-analytical solution of the Reynolds equation considering cavitation. International Journal of Mechanical Sciences 2023; 247: 108164. https://doi.org/10.1016/j.ijmecsci.2023.108164.
5. Xie S, Li Y, Tan H, Liu R, Zhang F. Multi-scale and multi-layer perceptron hybrid method for bearings fault diagnosis. International Journal of Mechanical Sciences 2022; 235: 107708. https://doi.org/10.1016/j.ijmecsci.2022.107708.
6. Bogue R. Sensors for condition monitoring: a review of technologies and applications. Sensor Review 2013; 33(4): 295–299. https://doi.org/10.1108/SR-05-2013-675.
7. Sicard B, Alsadi N, Spachos P, Ziada Y, Gadsden SA. Predictive Maintenance and Condition Monitoring in Machine Tools: An IoT Approach. 2022 IEEE International IOT, Electronics and Mechatronics Conference (IEMTRONICS). IEEE; 2022: 1–9. https://doi.org/10.1109/IEMTRONICS55184.2022.9795726.
8. Ghazizadeh A, Sarani M, Hamid M, Ghasemkhani A. Detecting and estimating the time of a single-step change in nonlinear profiles using artificial neural networks. International Journal of System Assurance Engineering and Management 2023; 14(1): 74–86. https://doi.org/10.1007/s13198-021-01121-y.
9. Bai R, Wang H, Sun W, Shi Y. Fault diagnosis method for rotating machinery based on SEDenseNet and Gramian Angular Field. Eksploatacja i Niezawodność – Maintenance and Reliability 2024; 26(1): 191445. https://doi.org/10.17531/ein/191445.
10. Lei X, Lu N, Jiang B, Wang C, Chen C. A Multi-scale Attention Mechanism Diagnosis Method with Adaptive Online Updating Based on Deep Learning under Variable Working Conditions. Eksploatacja i Niezawodność – Maintenance and Reliability 2024; 27(1): 192975. https://doi.org/10.17531/ein/192975.
11. Kozłowski E, Borucka A, Oleszczuk P, Leszczyński N. Evaluation of readiness of the technical system using the semi-Markov model with

selected sojourn time distributions. Eksploatacja i Niezawodność – Maintenance and Reliability 2024; 26(1): 191545. https://doi.org/10.17531/ein/191545.

12. Sobczuk S, Liniewski J, Borucka A. Diagnostics of production processes using selected Lean Manufacturing tools. Diagnostyka 2024; 25(1): 1–15. https://doi.org/10.29354/diag/190140.
13. Elkihel A, Abouelanouar B, Gziri H. Rotating Machines Energy Loss Due to Unbalance 2020; 684 :300–308. https://doi.org/10.1007/978-3-030-53187-4_34.
14. Drosińska-Komor M, Głuch J, Breńkacz Ł, Ziółkowski P. On the Use of Selected 4th Generation Nuclear Reactors in Marine Power Plants. Polish Maritime Research 2022; 29: 76–84. https://doi.org/10.2478/pomr-2022-0008.
15. Olszewski W, Dzida M, Nguyen V G, Cao D N. Reduction of CO 2 Emissions from Offshore Combined Cycle Diesel Engine-Steam Turbine Power Plant Powered by Alternative Fuels. Polish Maritime Research 2023; 30(3): 71–80. https://doi.org/10.2478/pomr-2023-0040.
16. Szturgulewski K, Głuch J, Drosińska-Komor M, Ziółkowski P, Gardzilewicz A, Brzezińska-Gołębiewska K. Hybrid geothermal-fossil power cycle analysis in a Polish setting with a focus on off-design performance and CO2 emissions reductions. Energy 2024; 299: 131382. https://doi.org/10.1016/j.energy.2024.131382.
17. Liu Y, Zhang M, Sun C, Hu M, Chen D, Liu Z, Tan J. A method to minimize stage-by-stage initial unbalance in the aero engine assembly of multistage rotors. Aerosp Sci Technol 2019; 85: 270–276. https://doi.org/10.1016/j.ast.2018.12.007.
18. Muszynska A. Rotordynamics. CRC Press; 2005. https://doi.org/10.1201/9781420027792.
19. Blaut J, Korbiel T, Batko W. Application of the teager-kaiser energy operator to detect instability of a plain bearing. Diagnostyka 2016; 17(2): 99–105.
20. Blaut J, Breńkacz Ł. Application of the Teager-Kaiser energy operator in diagnostics of a hydrodynamic bearing. Eksploatacja i Niezawodność – Maintenance and Reliability 2020; 22: 757–765. https://doi.org/10.17531/ein.2020.4.20.
21. Burdzik R, Konieczny Ł, Warczek J, Cioch W. Discussion on adaptation of linear decimation procedures for TFR analysis of non-stationary vibration signals of vehicle suspension. Mechanics Research Communications 2017;82:29–35. https://doi.org/10.1016/j.mechrescom.2016.11.002.
22. Antoniadou I, Manson G, Staszewski W J, Barszcz T, Worden K. A time–frequency analysis approach for condition monitoring of a wind turbine gearbox under varying load conditions. Mech Syst Signal Process 2015; 64-65: 188–216. https://doi.org/10.1016/j.ymssp.2015.03.003.
23. Song L, Wang H, Chen P. Step-by-Step Fuzzy Diagnosis Method for Equipment Based on Symptom Extraction and Trivalent Logic Fuzzy Diagnosis Theory. IEEE Transactions on Fuzzy Systems 2018; 26(6): 3467–78. https://doi.org/10.1109/TFUZZ.2018.2833820.
24. Hao Y, Song L, Cui L, Wang H. A three-dimensional geometric features-based SCA algorithm for compound faults diagnosis. Measurement 2019; 134: 480–491. https://doi.org/10.1016/j.measurement.2018.10.098.
25. Li Y, Li G, Yang Y, Liang X, Xu M. A fault diagnosis scheme for planetary gearboxes using adaptive multi-scale morphology filter and modified hierarchical permutation entropy. Mechanical Systems and Signal Processing 2018; 105: 319–337. https://doi.org/10.1016/j.ymssp.2017.12.008.
26. Pawlik P, Kania K, Przysucha B. Fault diagnosis of machines operating in variable conditions using artificial neural network not requiring training data from a faulty machine. Eksploatacja i Niezawodność – Maintenance and Reliability 2023; 25(2): 168109. https://doi.org/10.17531/ein/168109.
27. Breńkacz Ł, Żywica G, Bogulicz M. Selection of the oil-free bearing system for a 30 kW ORC microturbine. Journal of Vibroengineering 2019; 21(2): 318–330. https://doi.org/10.21595/jve.2018.19980.
28. Breńkacz Ł, Żywica G, Bogulicz M. Selection of the Bearing System for a 1 kW ORC Microturbine 2019; 60: 223–35. https://doi.org/10.1007/978-3-319-99262-4_16.
29. Żywica G, Breńkacz Ł, Bagiński P. Interactions in the Rotor-Bearings-Support Structure System of the Multi-stage ORC Microturbine. Journal of Vibration Engineering & Technologies 2018; 6(4): 369–377. https://doi.org/10.1007/s42417-018-0051-2.
30. Breńkacz L, Żywica G, Bogulicz M. Numerical Analysis of the Rotor of a 30 kW ORC Microturbine Considering Properties of Aerodynamic Gas Bearings. Mechanics and Mechanical Engineering 2018; 22(2): 425–435.

31. Rostaghi M, Ashory MR, Azami H. Application of dispersion entropy to status characterization of rotary machines. Journal of Sound and Vibration 2019; 438: 291–308. https://doi.org/10.1016/j.jsv.2018.08.025.
32. Mechanical vibration-Balance quality requirements for rotors in a constant (rigid) state. ISO 1940-1:2003. International Organization for Standardization; 2003.
33. Chung Y-H, Chen Y-L. Adaptive Vision-Based Method for Rotor Dynamic Balance System. IEEE Access 2021; 9: 22996–23006. https://doi.org/10.1109/ACCESS.2021.3055257.
34. Kozioł M, Cupiał P. The influence of the active control of internal damping on the stability of a cantilever rotor with a disc. Mechanics Based Design of Structures and Machines 2022; 50(2): 288–301. https://doi.org/10.1080/15397734.2020.1717965.
35. Kumar P, Tiwari R. Finite element modelling, analysis and identification using novel trial misalignment approach in an unbalanced and misaligned flexible rotor system levitated by active magnetic bearings. Mechanical Systems and Signal Processing 2021; 152: 107454. https://doi.org/10.1016/j.ymssp.2020.107454.
36. Breńkacz Ł. Dynwir S-70 program for modal analysis of multisupported and multimass rotors. Diagnostyka 2013; 14(3): 25–30.
37. Li Y, Long T, Luo Z, Wen C, Zhu Z, Jin L, Li B. Numerical and experimental investigations on dynamic behaviors of a bolted joint rotor system with pedestal looseness. Journal of Sound and Vibration 2024; 571: 118036. https://doi.org/10.1016/j.jsv.2023.118036.
38. Hao B. Symbolic dynamics and characterization of complexity. Physica D 1991; 51: 161–176. https://doi.org/10.1016/0167-2789(91)90229-3.
39. Zhang T, Chen Y, Chen Y. Hierarchical dispersion entropy and its application in fault diagnosis of rolling bearing. Journal of Vibroengineering 2022; 24(4): 862–870. https://doi.org/10.21595/jve.2022.22354.
40. Li Y, Tang B, Geng B, Jiao S. Fractional Order Fuzzy Dispersion Entropy and Its Application in Bearing Fault Diagnosis. Fractal and Fractional 2022; 6(10): 544. https://doi.org/10.3390/fractalfract6100544.
41. Blaut J, Breńkacz Ł. Application of the dispersion entropy with sliding window for the analysis of mechanical systems. Diagnostyka 2024; 25(2): 1–12. https://doi.org/10.29354/diag/195473.